

## COMMUNICATION

[View Article Online](#)  
[View Journal](#) | [View Issue](#)

Cite this: *Polym. Chem.*, 2022, **13**, 3981

Received 16th May 2022,  
Accepted 16th June 2022

DOI: 10.1039/d2py00629d

[rsc.li/polymers](https://rsc.li/polymers)

## Thioanhydride/isothiocyanate/epoxide ring-opening terpolymerisation: sequence selective enchainment of monomer mixtures and switchable catalysis†

Dorothee Silbernagl,<sup>a</sup> Heinz Sturm<sup>a</sup> and Alex J. Plajer<sup>a,b</sup>

**We report a new sequence selective terpolymerisation in which three monomers (butylene oxide (BO) A, PhNCS B and phthalic thioanhydride (PTA) C) are selectively enchainment into an (ABA'C)<sub>n</sub> sequence. PTA/PhNCS/BO ring-opening terpolymerisation ROTERP can be coupled with CS<sub>2</sub> ROTERP to generate tetrapolymers and with  $\epsilon$ DL ROP in switchable catalysis for blockpolymer synthesis.**

Heteroatom-containing polymers have strong potential as degradable replacements for polymers based on saturated aliphatic backbones.<sup>1–3</sup> Often such polymers are synthesised *via* the living ring opening polymerisation (ROP) of a heterocycle A to produce (A)<sub>n</sub> such as poly(thio)esters, poly(thio)carbonate and poly(thio)ethers.<sup>2,4</sup> In some cases, the ROP of three or four-membered heterocycles A can be coupled with the insertion of heteroallenes or cyclic anhydrides B to generate alternating copolymers (AB)<sub>n</sub> in so called ring-opening copolymerisation (ROCOP).<sup>5,6</sup> Prominent examples include CO<sub>2</sub>/epoxide ROCOP forming polycarbonates or cyclic anhydride/epoxide ROCOP forming polyesters.<sup>7–9</sup> However, sulfur-containing variants also exist and relevant to this study are recent reports on isothiocyanate/epoxide ROCOP forming poly(monothioimidocarbonates), isothiocyanate/thiirane ROCOP forming poly(dithioimidocarbonates), cyclic thioanhydride/epoxide ROCOP forming poly(ester-*alt*-thioesters).<sup>10–18</sup> Recently we realised alternating ring-opening terpolymerisation (ROTERP) of ternary monomer mixtures comprising thiophthalic anhydride (PTA), CS<sub>2</sub> and butylene oxide (BO).<sup>19</sup> Here, a simple lithium catalyst (*e.g.* lithiumbenzyloxide LiOBn or lithiumhexamethyldisilazide LiHMDS) selectively forms poly(ester-*alt*-ester-*alt*-trithiocarbonates) in up to 98% selectivity with respect to the

erroneous thioester links from PTA/BO ROCOP. The polymer shows an unusual “head-to-head-*alt*-tail-to-tail” selectivity, meaning that ester groups sit next to tertiary carbon centres while trithiocarbonates sit next to secondary carbon centres. Our results indicated that PTA/CS<sub>2</sub>/BO ROTERP formally derives from Li catalysed CS<sub>2</sub>/BO ROCOP reported by Werner and co-workers.<sup>17</sup> Both polymerisations are enabled by a O/S exchange reaction step in which an alkoxide chain end from a ring opened epoxide A isomerizes into a thiolate through incorporation of the oxygen into the adjacent link and this isomerised incorporated epoxide (forming a link akin insertion of a virtual thiirane) has been termed A'.<sup>17,20</sup> Thus, we hypothesised that other monomer combinations which undergo Li catalysed ROCOP could be suitable for sequence selective ROTERP. Xiong and coworkers very recently reported RNCS/epoxide ROCOP mediated by a simple LiO<sup>t</sup>Bu catalyst and accordingly we hypothesised that isothiocyanates could undergo ROTERP (Fig. 1).<sup>12</sup>

Therefore, we investigated the terpolymerisation of PTA/PhNCS/BO at different monomer ratios and catalyst loadings at 80 °C with lithiumbenzyloxide (LiOBn) as the catalyst (Table 1). Gratifyingly, we find that mixtures comprising 15 eq. PhNCS and 5 eq. BO with LiOBn loadings of 1–8 mol% per equivalent of PTA form poly(ester-*alt*-ester-*alt*-dithioimidocarbonates) in quantitative polymer selectivity. The <sup>1</sup>H NMR spectrum (Fig. 2) of the polymer shows two main aryl resonances corresponding to a symmetrically substituted terephthalate unit ( $\delta$  = 7.67 and 7.47 ppm) in an approximate 4 : 5 integrative ratio with respect to the NPh aromatic resonances indicating a 1 : 1 ratio of the two aromatic moieties.

Furthermore, there is one main resonance for the CHR<sub>3</sub> protons ( $\delta$  = 5.23 ppm) in a 2 : 4 integrative ratio and one main signal for the CH<sub>2</sub>R<sub>2</sub> protons ( $\delta$  = 3.80–2.90 ppm) in a 4 : 4 integrative ratio to the aromatic terephthalate signals respectively. The <sup>13</sup>C{<sup>1</sup>H} NMR spectrum (Fig. 2) reveals that the links formed are primarily dithioimidocarbonates R–S–C(=NPh)–S–R ( $\delta$  = 159.1 ppm,  $\approx$ 31% of all links) and arylesters R–C(=O)–O–R ( $\delta$  = 166.6 ppm,  $\approx$ 64% of all links), alongside minor thio-

<sup>a</sup>BAM Bundesanstalt für Materialforschung und -Prüfung, Unter den Eichen 87, 12205 Berlin, Germany

<sup>b</sup>Institut für Chemie und Biochemie, Freie Universität Berlin, Fabeckstraße 34–36, 14195 Berlin, Germany. E-mail: [plajer@zedat.fu-berlin.de](mailto:plajer@zedat.fu-berlin.de)

† Electronic supplementary information (ESI) available. See DOI: <https://doi.org/10.1039/d2py00629d>

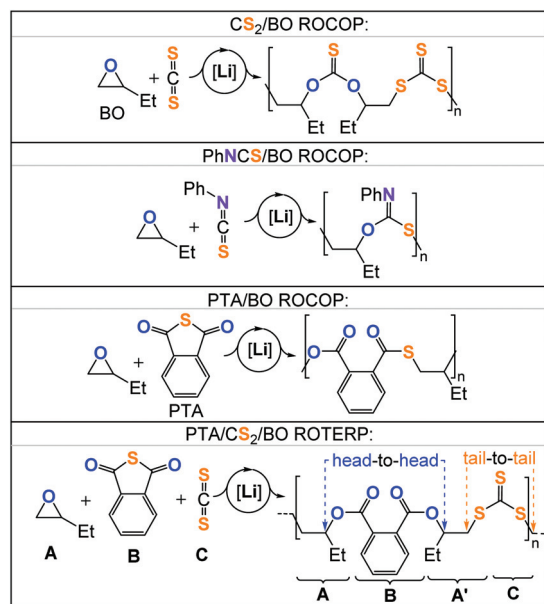


**Fig. 1** Comparison of different ROCOPs and ROTERP. [Li] = LiN(SiMe<sub>3</sub>) or LiOCH<sub>2</sub>Ph (LiOBn).<sup>12,17,19</sup>

ester R-C(=O)-S-R ( $\delta$  = 192.7 ppm,  $\approx$ 2.5% of all links) and monothioimidocarbonate R-O-C(=NPh)-S-R ( $\delta$  = 156.0 ppm,  $\approx$ 2.5% of all links) linkages (95% ROTERP links and 5% ROCOP errors). Due to overlapping <sup>1</sup>H NMR resonances for the respective linkages, the linkage ratios were approximated by integration of the relative integrals of the quaternary carbon resonances which proved to correspond well to the linkage ratios determined by integration of the <sup>1</sup>H NMR spectra in related terpolymers.<sup>19</sup> The thioester and monothioimidocarbonate links represent the links of the parent ROCOP reactions between PTA/BO and PhNCS/BO and are inferred to result from incomplete O/S exchange and insertion of PTA or PhNCS into alkoxide chain ends or from insertion of thiolate chain

ends into PTA as previously shown.<sup>19</sup> 2D NMR spectroscopy (Fig. S3 and S4†) further substantiates that dithioimidocarbonate units are positioned adjacent to CH<sub>2</sub> groups while arylesters are connected to the tertiary CHMe groups. Hence, we propose a similar “head-to-head-*alt*-tail-to-tail” selectivity connectivity as for the previously reported ROTERP involving CS<sub>2</sub> in place of PhNCS. Furthermore, no ether links were detected in the polymer, which are a common side products formed in related ROCOPs.<sup>5,21</sup> The respective resonance ratios remain unchanged after multiple precipitations from DCM:MeOH or THF:pentane confirming that all links are part of the same polymer. Linkage identity could be further substantiated by the ATR-IR spectrum (Fig. 2) showing an arylester C=O stretch at  $\tilde{\nu}$  = 1716 cm<sup>-1</sup> as well as a dithioimidocarbonate C=N stretch at  $\tilde{\nu}$  = 1563 cm<sup>-1</sup>.<sup>10,19</sup> MALDI-TOF analysis unfortunately only led to decomposition of the materials and no signals could be identified as previously reported for sulfur-rich polymers.<sup>22,23</sup> However the OBn initiator can be identified to be part of the purified polymers (Fig. S5†) suggesting the formation of linear as opposed to cyclic chains. The polymers are colourless amorphous solids ( $T_g$  = 30.6 °C, Fig. S8†) with good thermal stability ( $T_{d,5\%}$  = 230.1 °C, Fig. S10†). SEC analysis of the obtained materials at catalyst loadings of 1–8 mol% vs. PTA shows that the methodology can yield polymers with molecular weights ranging from  $M_n$  = 2.55 to 14.00 kg mol<sup>-1</sup> ( $D$  = 1.15–1.49, Table 1 and Fig. S19†). Attempting lower LiOBn loadings did not result in any polymerisation. Employing Na or K in place of Li resulted in unappreciable turnover supporting that Li acts as a catalyst rather than a spectator counteranion for the OBn initiator (Table 1 run #9 and #10). Decreasing the amount of PhNCS in the initial monomer mixture (and therefore increasing the PTA concentration as PhNCS acts as a cosolvent) led to more erroneous thioester links (Table 1 run #6–#8) and a similar amount of monothioimidocarbonate links (*ca.* 3% of all links). This can be rationalized by kinetic competition between O/S

**Table 1** ROTERP Polymerisation data

LiOBn : PTA : BO : PhNCS <sup>a</sup>	Time [min]	PTA conversion <sup>b</sup>	Coupling selectivity <sup>c</sup>	Ester selectivity <sup>d</sup>	$M_n$ , <sup>e</sup> [kDa] ( $D$ )
1 : 6 : 32 : 93	2	99%	>99%	97.5%	2.51 (1.15)
1 : 13 : 62 : 187	3	98%	>99%	97.5%	5.5 (1.17)
1 : 25 : 125 : 375	6	98%	>99%	97.5%	9.94 (1.20)
1 : 50 : 250 : 750	30	95%	>99%	97.5%	13.61 (1.33)
1 : 100 : 500 : 1500	480	86%	>99%	97.5%	14.0 (1.49)
1 : 50 : 250 : 125	30	>99%	>99%	91%	22.18 (1.32)
1 : 50 : 250 : 250	30	>99%	>99%	94%	21.6 (1.29)
1 : 50 : 250 : 500	30	>99%	>99%	95%	17.61 (1.28)
1 : 50 : 250 : 750 <sup>f</sup>	30	10%	>99%	n.d.	n.d.
1 : 50 : 250 : 750 <sup>g</sup>	30	0%	—	—	—
1 : 50 : 250 : 375 : 375 <sup>h</sup>	30	>99%	95%	96%	18.09 (1.38)

<sup>a</sup> Copolymerisation at  $T$  = 80 °C, LiOBn generated *in situ* from LiHMDS and BnOH (see ESI†). <sup>b</sup> Determined by comparison of the relative integrals, in the normalised <sup>1</sup>H NMR spectrum (CDCl<sub>3</sub>, 25 °C, 400 MHz), of terephthalate CH resonances due to (co/ter)polymer and PTA. <sup>c</sup> Determined by comparison of the relative integrals, in the normalised <sup>1</sup>H NMR spectrum (CDCl<sub>3</sub>, 25 °C, 400 MHz), of tertiary CH resonances due to (co/ter)polymer and cyclic thioimidocarbonate and polyether. <sup>d</sup> Determined by comparison of the relative integrals, in the normalised the <sup>13</sup>C{<sup>1</sup>H} NMR spectrum (CDCl<sub>3</sub>, 25 °C) of resonances due to ester relative to thioester links. <sup>e</sup> Determined by SEC (size-exclusion chromatography) measurements conducted in THF, using narrow MW polystyrene standards to calibrate the instrument. <sup>f</sup> NaHMDS was employed in place of LiHMDS. <sup>g</sup> KHMDS was employed in place of LiHMDS. <sup>h</sup> CS<sub>2</sub>.



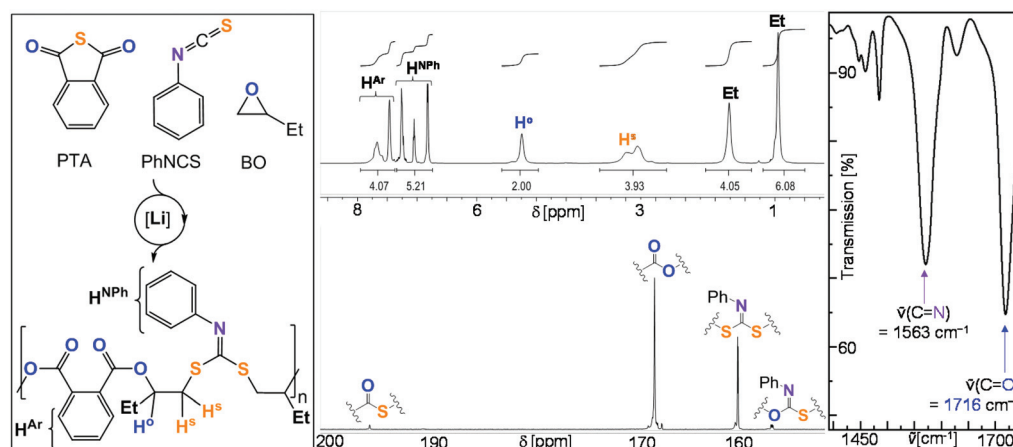
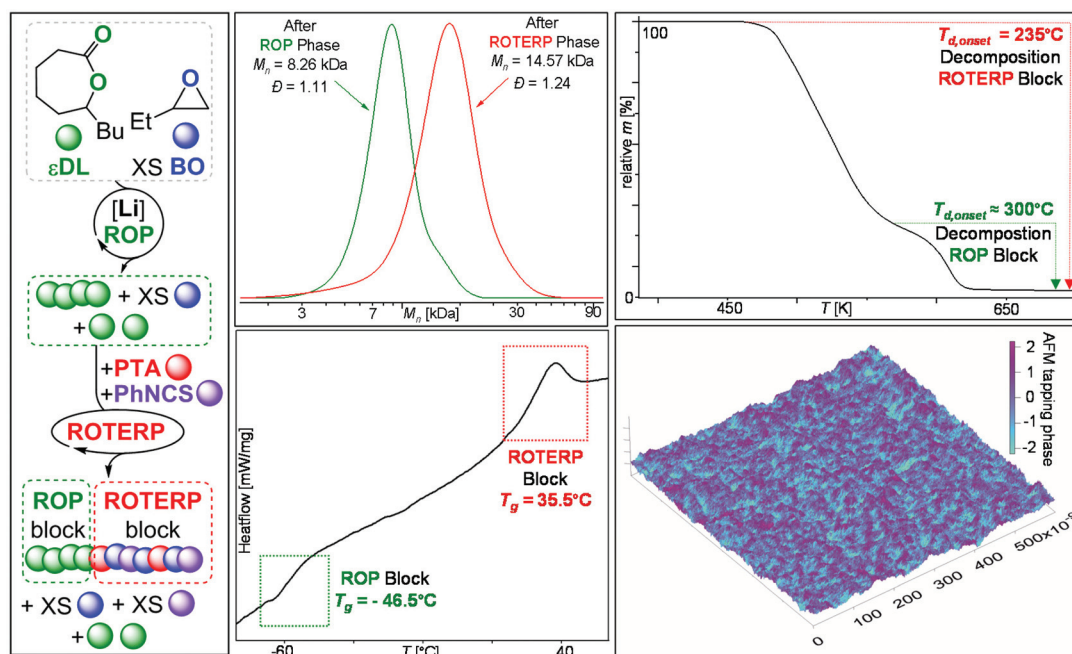


Fig. 2 Reaction Scheme,  $^1\text{H}$ ,  $^{13}\text{C}\{^1\text{H}\}$  NMR and IR spectra of PTA/PhNCS/BO terpolymer (polymer of Table 1, run #4).

rearrangement and propagation from alkoxide intermediates. In these cases, we also observe the onset of PhNCS/BO ROCOP to form poly(monothioimidocarbonates) once all PTA is consumed as confirmed by  $^1\text{H}$  (Fig. S6†) and  $^{13}\text{C}$  NMR (Fig. S7†) spectroscopy. This leads to poly(monothioimidocarbonate) blocks forming adjacent to the ROTERP blocks which also explains the higher molecular weights obtained at the same PTA loadings. The new monomer combination is furthermore compatible with PTA/ $\text{CS}_2$ /BO ROTERP. Tetrapolymerisation of PTA and BO with PhNCS and  $\text{CS}_2$  results in poly(ester-alt-ester-alt-heterocarbonate) formation in which both RNCS (forming dithioimidocarbonates) and  $\text{CS}_2$  (forming trithiocarbonates) are incorporated into the polymer. NMR (Fig. S11–S15†) and FTATR-IR (Fig. S17†) clearly show the presence of trithiocarbonate ( $\delta = 222.8$  ppm,  $\tilde{\nu} = 1063$   $\text{cm}^{-1}$ ) links in addition to the other links from PTA/PhNCS/BO ROTERP. Corresponding to Table 1 run #11, a polymer comprising 67% arylester, 23% trithiocarbonate, 6% dithioimidocarbonate, 3.5% thioester and 0.5% monothioimidocarbonate links is produced (96% ROTERP links and 4% ROCOP errors). Apparently, PTA/PhNCS/BO ROTERP follows a similar polymerisation mechanism (Fig. S31†) as the one proposed for PTA/ $\text{CS}_2$ /BO ROTERP. It involves a central O/S rearrangement step and preferential insertion of PTA into alkoxide chain ends and of the heteroallene into thiolate chain ends at which point a mixture of heteroallenes can be employed which are then both incorporated at this insertion step. Interestingly, although PhNCS and  $\text{CS}_2$  are employed in an equimolar ratio,  $\text{CS}_2$  is incorporated preferentially in 77% selectivity. We could confirm this observation by varying the initial PhNCS: $\text{CS}_2$  ratio in which  $\text{CS}_2$  was always incorporated to a greater degree than employed in the initial monomer feed (see Fig. S18†). In ROCOP, switchable catalysis has been established as an elegant and valuable tool to synthesise blockpolymers with useful material properties.<sup>24–26</sup> Here a suitable catalyst first mediates the ROP of for example cyclic esters (e.g.  $\epsilon\text{DL}$  forming PDL) with epoxides present in the mixture until the second ROCOP monomer (e.g.  $\text{CO}_2$ ) is

added causing immediate termination of ROP and the onset of (e.g.  $\text{CO}_2$ /epoxide forming polycarbonate) ROCOP to form a ROCOP block connected to the ROP polymer. We recently showed that ROTERP is also suitable for switchable catalysis in combination with the lithium catalysed ROP of  $\epsilon\text{DL}$ .<sup>19</sup> Having identified a new heteroallene that undergoes ROTERP, we were intrigued whether this monomer combination is also suitable for the construction of blockpolymers *via* switchable catalysis. Accordingly, we added PhNCS (750 eq. per LiOBn) and PTA (50 eq.) to polymerising  $\epsilon\text{DL}$  (50 eq.) in BO (250 eq.) after 15 min at room temperature which completely and immediately stops the occurrence of  $\epsilon\text{DL}$  ROP. Heating to 80  $^\circ\text{C}$  initiates ROTERP and a poly(ester-alt-ester-alt-dithioiminocarbonate) block grows from the PDL-chain-end until the reaction is stopped after 30 min. Under these conditions the ROTERP block consists of 64% arylester links, 31% dithioimidocarbonate links and 2.5% erroneous thioester and monothioimidocarbonate links, respectively (95% ROTERP links and 5% ROCOP errors). Switchable catalysis and block polymer formation were established by various methods: (i) no  $\epsilon\text{DL}$  is consumed after ROTERP starts (Fig. S21†) and the  $^{13}\text{C}\{^1\text{H}\}$  PDL ( $\delta = 173.2$  ppm, Fig. S23†) remains unchanged showing that ROP stops and that no transesterification between blocks occurs; (ii) the number averaged molecular weight shifts from  $M_n = 8.26$  ( $D = 1.11$ ) to 14.57  $\text{kg mol}^{-1}$  ( $D = 1.24$ , Fig. 3), which shows the growth of existing chains rather than the initiation of new ones; (iii)  $^{31}\text{P}$  end group analysis shows the consumption of all PDL end groups (Fig. S30†);<sup>27</sup> (iv) the composition of the resulting blockpolymer remains unchanged through multiple precipitations from DCM/MeOH and THF/pentane supporting that the blocks are joint; (vii) DSC analysis exhibits two  $T_g$ 's at  $-46.5$   $^\circ\text{C}$  for the ROP block and 35.5  $^\circ\text{C}$  for the ROTERP block suggesting microphase separation in the solid-state which could be confirmed by AFM (Fig. 3);<sup>28</sup> (viii) TGA analysis shows a stepwise thermal decomposition profile with two  $T_{d,\text{onset}}$  at approximately 235  $^\circ\text{C}$  for the ROTERP block and 300  $^\circ\text{C}$  for the ROP block (Fig. 3). In conclusion, we have identified a new





**Fig. 3** (Left)  $\epsilon$ DL ROP to ROTERP switchable catalysis sequence. (Right) overlaid SEC traces before and after switch as well as TGA, DSC and 3d image of AFM tapping topography (height range 4 nm) of the obtained blockpolymer. 3d display of topography is overlaid with a false colour map of the AFM tapping phase which differentiates between the blockpolymer's components.

monomer combination that undergoes lithium catalysed sequence selective terpolymerisation. Mixtures of PTA/PhNCS/BO forming poly(ester-alt-ester-alt-dithioimidocarbonate)s in up to 95% selectivity with respect to the erroneous links from PhNCS/BO and PTA/BO ROCOP. This has enabled the synthesis of complex tetrapolymers from quarternary monomer mixture or *via* switchable catalysis. Our results establish ROTERP as a valuable methodology for the synthesis of heteroatom containing blockpolymers.

## Conflicts of interest

There are no conflicts of interests.

## Acknowledgements

The VCI is acknowledged for a Liebig Fellowship for A. J. P. Prof. Dr Christian Müller and Prof. Dr Rainer Haag are thanked for continuous support. Thomas Rybak and Prof. Dr Bernhard Schartel are thanked for DSC measurements.

## Notes and references

- Y. Zhu, C. Romain and C. K. Williams, *Nature*, 2016, **540**, 354–362.
- G. Becker and F. R. Wurm, *Chem. Soc. Rev.*, 2018, **47**, 7739–7782.
- T. P. Haider, C. Völker, J. Kramm, K. Landfester and F. R. Wurm, *Angew. Chem., Int. Ed.*, 2019, **58**, 50–62.
- N. E. Kamber, W. Jeong, R. M. Waymouth, R. C. Pratt, B. G. G. Lohmeijer and J. L. Hedrick, *Chem. Rev.*, 2007, **107**, 5813–5840.
- A. J. Plajer and C. K. Williams, *Angew. Chem., Int. Ed.*, 2022, DOI: [10.1002/anie.202104495](https://doi.org/10.1002/anie.202104495).
- S. Paul, Y. Zhu, C. Romain, R. Brooks, P. K. Saini and C. K. Williams, *Chem. Commun.*, 2015, **51**, 6459–6479.
- J. M. Longo, M. J. Sanford and G. W. Coates, *Chem. Rev.*, 2016, **116**, 15167–15197.
- B. Grignard, S. Gennen, C. Jérôme, A. W. Kleij and C. Detrembleur, *Chem. Soc. Rev.*, 2019, **48**, 4466–4514.
- C. M. Kozak, K. Ambrose and T. S. Anderson, *Coord. Chem. Rev.*, 2018, **376**, 565–587.
- X.-F. Zhu, R. Xie, G.-W. Yang, X.-Y. Lu and G.-P. Wu, *ACS Macro Lett.*, 2021, **10**, 135–140.
- T. Lai, P. Zhang, J. Zhao and G. Zhang, *Macromolecules*, 2021, **54**, 11113–11125.
- L. Song, M. Liu, D. You, W. Wei and H. Xiong, *Macromolecules*, 2021, **54**, 10529–10536.
- C. Chen, Y. Gnanou and X. Feng, *Macromolecules*, 2021, **54**, 9474–9481.
- X.-F. Zhu, G.-W. Yang, R. Xie and G.-P. Wu, *Angew. Chem., Int. Ed.*, 2022, DOI: [10.1002/anie.202115189](https://doi.org/10.1002/anie.202115189).
- L.-Y. Wang, G.-G. Gu, B.-H. Ren, T.-J. Yue, X.-B. Lu and W.-M. Ren, *ACS Catal.*, 2020, **10**, 6635–6644.





- 16 L.-Y. Wang, G.-G. Gu, T.-J. Yue, W.-M. Ren and X.-B. Lu, *Macromolecules*, 2019, **52**, 2439–2445.
- 17 J. Diebler, H. Komber, L. Häußler, A. Lederer and T. Werner, *Macromolecules*, 2016, **49**, 4723–4731.
- 18 T.-J. Yue, M.-C. Zhang, G.-G. Gu, L.-Y. Wang, W.-M. Ren and X.-B. Lu, *Angew. Chem., Int. Ed.*, 2019, **58**, 618–623.
- 19 S. M. Rupf, P. Pröhm and A. J. Plajer, *Chem. Sci.*, 2022, **13**, 6355–6365.
- 20 J. Diebler, A. Spannenberg and T. Werner, *Org. Biomol. Chem.*, 2016, **14**, 7480–7489.
- 21 A. J. Plajer and C. K. Williams, *Angew. Chem., Int. Ed.*, 2021, **60**, 13372–13379.
- 22 T. M. McGuire and A. Buchard, *Polym. Chem.*, 2021, **12**, 4253–4261.
- 23 W.-M. Ren, J.-Y. Chao, T.-J. Yue, B.-H. Ren, G.-G. Gu and X.-B. Lu, *Angew. Chem., Int. Ed.*, 2022, DOI: [10.1002/anie.202115950](https://doi.org/10.1002/anie.202115950).
- 24 A. C. Deacy, G. L. Gregory, G. S. Sulley, T. T. D. Chen and C. K. Williams, *J. Am. Chem. Soc.*, 2021, **143**, 10021–10040.
- 25 C. Romain and C. K. Williams, *Angew. Chem., Int. Ed.*, 2014, **53**, 1607–1610.
- 26 C. Hu, X. Pang and X. Chen, *Macromolecules*, 2022, **55**, 1879–1893.
- 27 A. Spyros, D. S. Argyropoulos and R. H. Marchessault, *Macromolecules*, 1997, **30**, 327–329.
- 28 F. S. Bates, M. A. Hillmyer, T. P. Lodge, C. M. Bates, K. T. Delaney and G. H. Fredrickson, *Science*, 2012, **336**, 434–440.

